Research Square

Preprints are preliminary reports that have not undergone peer review.
They should not be considered conclusive, used to inform clinical practice,
or referenced by the media as validated information.

Safety of Anchor Placement in Anterior Talofibular Ligament Repair: A Virtual Three-Dimensional Bone Model Study in Adults

Zhi-Xuan Xu
Affiliated Renhe Hospital of China Three Gorges University
Jie Wang
Affiliated Renhe Hospital of China Three Gorges University
Ming-Liang Chen
Affiliated Renhe Hospital of China Three Gorges University
Cheng-Yi Gu
Affiliated Renhe Hospital of China Three Gorges University
Xiang-Quan Cai
Affiliated Renhe Hospital of China Three Gorges University
Bo Li
Affiliated Renhe Hospital of China Three Gorges University
You Zhou
zhouyou8010@163.com

Affiliated Renhe Hospital of China Three Gorges University

Research Article

Keywords: anterior talofibular ligament, ankle instability, suture anchor, three-dimensional reconstruction, computed tomography

Posted Date: November 5th, 2026

DOI: https://doi.org/10.21203/rs.3.rs-11271011/v1

License: This work is licensed under a Creative Commons Attribution 4.0 International License.
Read Full License

Additional Declarations: No competing interests reported.

Abstract

Objective

To analyze the optimal position, safe angle, risk of fibular fossa penetration, and effective intraosseous fixation length for fibular-sided anchor placement during anterior talofibular ligament (ATFL) repair using virtual three-dimensional (3D) bone models.

Methods

We retrospectively enrolled 100 adults (59 males, 41 females) who underwent ankle CT and generated virtual 3D bone reconstructions. The ATFL fibular footprint center was defined as the anchor insertion point. A simulated 3.0 mm-diameter tunnel measured: (1) vertical distance from the insertion point to the fibular tip horizontal plane (h), (2) maximum angle (θ) in the sagittal plane avoiding fibular fossa penetration, and (3) effective tunnel length at 60°, 45°, and 30° parallel to the fibular sagittal plane and along the lateral malleolar ridge.

Results

Mean h was 5.36 ± 1.29 mm, and mean θ was 67.48 ± 8.05°. Effective tunnel lengths increased as insertion angle decreased. In the sagittal plane, effective lengths at 60°, 45°, and 30° were 17.99 ± 3.67, 22.09 ± 2.32, and 26.74 ± 2.75 mm, respectively; values along the lateral malleolar ridge were 17.58 ± 2.01, 19.62 ± 2.20, and 23.96 ± 2.84 mm. Fibular fossa penetration (11.0%) occurred only during 60° insertion parallel to the sagittal plane. Males exhibited significantly greater h values and effective tunnel lengths than females ($P < 0.001$); θ did not differ between sexes ($P = 0.632$).

Conclusion

The optimal fibular-sided anchor insertion point is located approximately 5.4 mm proximal to the fibular tip. Insertion parallel to the fibular sagittal plane at 30°–45° balances safety and intraosseous fixation length. When a larger insertion angle is necessitated, insertion along the lateral malleolar ridge direction may be a safer alternative. Anchor length selection should account for sex differences, with lengths not exceeding 20 mm for males and 18 mm for females.

Introduction

For patients with lateral ankle ligament injuries who remain symptomatic after at least six months of systematic conservative treatment, surgical intervention is essential for restoring ankle stability and functional recovery[1–3]. The anterior talofibular ligament (ATFL) is the primary ligament addressed in the surgical management of chronic lateral ankle instability. Current surgical options include anatomical

repair—principally the Broström procedure and its modifications—and anatomical reconstruction using autograft or allograft tendons[4, 5]. The Broström procedure restores stability by directly repairing and imbricating the attenuated ligament, whereas the modified Broström-Gould technique augments the repair with the inferior extensor retinaculum for enhanced outcomes[1, 5]. Recently, arthroscopic Broström repair, suture tape augmentation, and individualized reinforcement strategies have gained increasing adoption, and comparative studies of open versus arthroscopic techniques as well as the selection of indications have become active areas of investigation[1, 5–10].

During ATFL repair, the position, direction, and depth of anchor placement critically influence surgical safety, fixation quality, and complication risk. The distal fibula offers limited bone stock within a confined anatomical space. The fibular fossa lies posteriorly, and the peroneus longus and brevis tendons, the sural nerve, and associated vascular structures are in close proximity. Inappropriate anchor positioning or angulation may result in posterior cortical breach and tendon irritation, causing postoperative pain and mechanical impingement. Furthermore, anchor penetration into the fibular fossa may compromise fixation and potentially lead to repair failure[11–14]. Thus, the safety of fibular-sided anchor placement is a key technical determinant of ATFL repair quality.

Although previous studies have examined safe angles and depths for anchor placement in adult ATFL repair, systematic evaluation of insertion angles and quantitative measurement of effective tunnel lengths across different angles remain inadequate. The present study focused on the commonly reported insertion angles of 60°, 45°, and 30°, utilizing adult ankle CT data to construct virtual 3D bone models for systematic measurement of anchor insertion parameters across different directions and angles[11, 15–18]. The aim of this study was to analyze the optimal insertion position, risk of fibular fossa penetration, and achievable effective intraosseous fixation length, thereby providing a reference for safe anchor placement and individualized surgical planning in ATFL repair.

Subjects and Methods

1.1 Study Subjects

This retrospective imaging measurement study enrolled adult patients who underwent ankle CT at our institution between January 2018 and January 2026.

Inclusion criteria

(1) age 18–50 years, skeletally mature; (2) ankle CT performed in the neutral position at our institution; (3) no bony structural injuries around the ankle; (4) no deformity or prior surgery of the foot or lower limb; (5) no osteochondral lesions of the talus or periarticular cystic bone lesions; (6) CT image quality adequate for 3D reconstruction and measurement.

Exclusion criteria

(1) concurrent fractures or vascular, nerve, or tendon injuries around the ankle; (2) prior ankle surgery; (3) inadequate CT image quality precluding reliable measurement; (4) systemic diseases affecting bone metabolism; (5) ankle osteoarthritis, rheumatoid arthritis, or other articular disorders.

A total of 100 patients (100 ankles) were included (59 males, 41 females). This study was approved by the Ethics Committee of our hospital (Approval No.: RH-2025-EX-022). As a retrospective study, the requirement for informed consent was waived. Clinical trial number: not applicable.

1.2 Imaging Data Acquisition and Virtual 3D Reconstruction

Imaging acquisition: All CT scans were performed on a Philips Ingenuity 128-slice spiral CT scanner with the following parameters: tube voltage 120 kV, tube current 150 mA, slice thickness 0.5 mm, and pitch 0.5 mm. Raw DICOM data were exported for subsequent analysis.

Virtual 3D reconstruction: DICOM data were imported into Mimics Research 21.0 software (Materialise NV, Leuven, Belgium). The 3D ankle model was extracted using threshold segmentation (bone tissue range: 228–3071 HU) and region growing tools. Editing tools were then applied to remove irrelevant noise while preserving all bony structures, yielding high-precision virtual 3D bone models. To standardize the measurement reference system, the line connecting the midpoints of the proximal and distal fibula was defined as the fibular longitudinal axis, and the plane perpendicular to this axis passing through the most distal fibular point was defined as the fibular tip horizontal plane.

1.3 Anchor Insertion Simulation and Measurement Parameters

Insertion point localization

Based on the anatomical studies by Matsui et al.[19, 20] and Fujishiro et al.[21], the bony prominence at the intersection of the anterior and inferior borders of the distal fibula was identified as the fibular obscure tubercle (FOT). The ATFL fibular footprint center is typically located 3–4 mm proximal to the FOT. On the reconstructed 3D models, the center of the ATFL anatomical attachment on the anteroinferior aspect of the lateral malleolus was determined as the anchor insertion point (Point X, Fig. 1) using anatomical landmarks.

Tunnel simulation

A cylinder with a diameter of 3.0 mm was used to simulate the anchor tunnel, consistent with clinically common anchor specifications. Different insertion angles were simulated by adjusting the cylinder orientation.

Figure 1 Lateral view of the distal fibula. The fibular anchor tunnels were designed at angles of 30°, 45°, and 60° relative to the fibular longitudinal axis, respectively. Point X, anchor insertion point; FOT, fibular

obscure tubercle; h, vertical distance from the insertion point to the fibular tip horizontal plane; dashed line, fibular tip horizontal plane

Measurement parameters and definitions:

All measurements were performed in Mimics software by two trained orthopedic surgeons, each performing two independent measurements. Mean values were used for analysis. If discrepancies exceeded 0.5 mm or 1°, a third senior orthopedic surgeon adjudicated, and the final value was determined by consensus. The specific parameters were as follows:

Vertical distance from the insertion point to the fibular tip horizontal plane, h (mm)

The perpendicular distance from Point X to the fibular tip horizontal plane (Fig. 1).

Tunnel length at different angles (mm): The theoretical bone tunnel length from the insertion point to the contralateral cortical exit. Two directions were measured: one parallel to the fibular sagittal plane (unmarked in text) and the other along the lateral malleolar ridge (denoted “a”). Both were measured at 60°, 45°, and 30° relative to the fibular longitudinal axis (Fig. 2a).

Effective tunnel length (mm)

The net intraosseous fixation length after subtracting bone loss from the 3.0 mm drill diameter at the entrance and exit. Fibular fossa penetration, if present, was recorded (Fig. 2b).

Maximum safe angle θ (°) in the sagittal plane

Within the sagittal plane containing the insertion point, the tunnel angle was incrementally adjusted until the tunnel edge reached the fibular fossa boundary. The maximum angle between the tunnel centerline and the fibular longitudinal axis at which the posterior tunnel remained entirely within the fibula without fossa penetration was recorded as θ (Fig. 2c–d).

1.4 Statistical Analysis

Statistical analysis was performed using SPSS 26.0. Normality of continuous variables was assessed with the Shapiro–Wilk test. Normally distributed data are presented as mean ± standard deviation (SD). Inter- and intra-observer reliability was evaluated using the intraclass correlation coefficient (ICC), with ICC > 0.75 indicating good agreement. Sex-based comparisons were performed using the independent-samples t-test. Categorical data are reported as frequencies and compared using the χ^2 test. Statistical significance was set at $P < 0.05$.

Results

2.1 General Characteristics

A total of 100 patients were enrolled (59 males, 41 females). Mean age was 33.08 ± 9.09 years (range: 18–50). There were 44 left and 56 right ankles. No significant differences existed between males and females in age (32.44 ± 8.65 vs. 34.00 ± 9.72 years, P = 0.402) or laterality (left/right: 30/29 vs. 14/27, P = 0.098), indicating good comparability between the two groups in these baseline characteristics. Height, weight, and body mass index were significantly greater in males (all P < 0.001) (Table 1).

Table 1
Comparison of baseline characteristics between male and female patients

Group	***n***	**Age (mean ± SD,years)**	**Laterality (Left/Right,n)**	**Height (mean ± SD,m)**	**Weight (mean ± SD, kg)**	**Body Mass Index (mean ± SD, kg/m²)**
Male	59	32.44 ± 8.65	30/29	1.70 ± 0.06	65.51 ± 9.90	22.65 ± 2.31
Female	41	34.00 ± 9.72	14/27	1.56 ± 0.04	50.33 ± 5.77	20.61 ± 2.84
Statistic		t=-0.825	χ^2=2.738	t = 19.415	t = 13.248	t = 5.573
P		0.402	0.098	< 0.001	< 0.001	< 0.001
P < 0.05 indicates statistical significance						

2.2 Reliability Analysis

Inter-observer reliability was assessed using a two-way random-effects model. ICC values ranged from 0.856 to 0.938 across all parameters, with values of 0.912 for h and 0.903 for θ. ICC for tunnel lengths at different angles ranged from 0.867 to 0.938. Intra-observer ICC ranged from 0.842 to 0.891, all exceeding 0.75. Overall, the measurements in this study demonstrated good stability and high data credibility.

2.3 Anatomical Parameter Measurements

The mean h was 5.36 ± 1.29 mm (range: 2.97–10.14 mm; median: 5.30 mm) (Table 2), indicating that the optimal insertion point is located approximately 5.4 mm proximal to the fibular tip.

The analysis of the maximum safe angle θ in the sagittal plane is presented in Table 2. Valid θ measurements were obtained in 78 specimens, with a mean of 67.48 ± 8.05° (range: 49.29°–83.55°). In the remaining 22 specimens, fibular fossa penetration did not occur even at 90°, indicating greater bony accommodation in some individuals. These were treated as censored data. A sensitivity analysis assigning 90° to censored cases yielded an overall mean θ of 72.43 ± 11.76° (males: 73.67 ± 12.51°; females: 70.63 ± 10.51°), with the sex-based difference remaining non-significant (t = 1.274, P = 0.206).

Table 2
Descriptive statistics of anatomical parameters

Parameter	*n*	Mean ± SD	Median	Minimum	Maximum
h(mm)	100	5.36 ± 1.29	5.30	2.97	10.14
θ(°)	78	67.48 ± 8.05	67.77	49.29	83.55

The valid sample size for parameter θ was 78. In the remaining 22 cases (22%), fibular fossa penetration did not occur even at an angle of 90° relative to the fibular longitudinal axis in the sagittal plane

2.4 Tunnel Lengths and Effective Fixation Lengths at Different Angles

Tunnel lengths and effective tunnel lengths at each angle and direction are detailed in Table 3. Both parameters increased as the insertion angle decreased from 60° to 30° in both directions. In the sagittal plane direction, effective tunnel lengths at 60°, 45°, and 30° were 17.99 ± 3.67 mm, 22.09 ± 2.32 mm, and 26.74 ± 2.75 mm, respectively, with corresponding total tunnel lengths of 20.33 ± 2.26 mm, 24.05 ± 2.24 mm, and 29.66 ± 2.84 mm. Along the lateral malleolar ridge, effective tunnel lengths were 17.58 ± 2.01 mm, 19.62 ± 2.20 mm, and 23.96 ± 2.84 mm, with total tunnel lengths of 20.01 ± 1.86 mm, 22.64 ± 2.01 mm, and 28.57 ± 2.71 mm. Reducing the insertion angle is favorable for achieving longer bony tunnels and greater intraosseous fixation lengths.

At equivalent angles, the sagittal plane direction consistently yielded greater tunnel lengths than the lateral malleolar ridge direction. At 45°, the effective tunnel length was 22.09 ± 2.32 mm versus 19.62 ± 2.20 mm; at 30°, the values were 26.74 ± 2.75 mm versus 23.96 ± 2.84 mm, respectively. This suggests that, under the same angle conditions, the sagittal plane direction is more advantageous for achieving longer intraosseous fixation lengths.

Table 3
Tunnel lengths and effective tunnel lengths at different angles: mean and standard deviation (mm)

Angle relative to the fibular longitudinal axis	Tunnel length	Effective tunnel length	*n*
60°	20.33 ± 2.26	17.99 ± 3.67	100
60°(a)	20.01 ± 1.86	17.58 ± 2.01	100
45°	24.05 ± 2.24	22.09 ± 2.32	100
45°(a)	22.64 ± 2.01	19.62 ± 2.20	100
30°	29.66 ± 2.84	26.74 ± 2.75	100
30°(a)	28.57 ± 2.71	23.96 ± 2.84	100

"a" indicates the insertion direction along the lateral malleolar ridge; the absence of "a" indicates the insertion direction parallel to the fibular sagittal plane containing the insertion point

The incidence of fibular fossa penetration at different drilling angles is presented in Table 4. Fibular fossa penetration occurred only during 60° insertion parallel to the sagittal plane (11 cases, 11.0%). No penetration was observed at 60°(a), 45°, 45°(a), 30°, or 30°(a). Among the insertion conditions evaluated in this study, larger angles—particularly 60° insertion parallel to the sagittal plane—carried a relatively higher risk of fibular fossa penetration. These findings indicate that while the lateral malleolar ridge direction provides slightly shorter effective tunnel lengths, it offers superior safety against fossa penetration.

Table 4
Incidence of fibular fossa penetration at different drilling angles

Angle relative to the fibular longitudinal axis	**Penetrations (*n*)**	**Total (*n*)**	**Incidence (%)**
60°	11	100	11.0
All other angles	0	100	0.0

"60°" refers to the insertion direction parallel to the fibular sagittal plane; "All other angles" include 60°(a) (lateral malleolar ridge direction), 45°, 45°(a), 30°, and 30°(a).

2.5 Sex-Based Comparison

Comparison of measurement parameters between male and female patients (Tables 5 and 6) revealed the following: males had a significantly greater insertion height h than females (5.82 ± 1.29 mm vs. 4.71 ± 0.99 mm; t = 4.640, P < 0.001), reflecting larger distal fibular dimensions and a higher ATFL footprint position in males. The θ value did not differ significantly between sexes (67.06 ± 8.12° vs. 67.94 ± 8.07°; t = − 0.480, P = 0.632), suggesting that the safe angle range for insertion is generally not affected by sex. Effective tunnel lengths were significantly greater in males at all angles (all P < 0.001). Overall, the intraosseous fixation length achievable in the distal fibula was greater in males than in females.

Table 5
Results of independent-samples *t*-test for anatomical parameters by sex

Parameter	**Male (mean ± SD)**	**Male (*n*)**	**Female (mean ± SD)**	**Female (*n*)**	***t***	***P***
h(mm)	5.82 ± 1.29	59	4.71 ± 0.99	41	4.640	< 0.001
θ(°)	67.06 ± 8.12	42	67.94 ± 8.07	36	-0.480	0.632

P < 0.05 indicates statistical significance. For parameter θ, valid measurements were obtained from 42 males and 36 females.

Table 6
Results of independent-samples *t*-test for effective tunnel lengths at different angles by sex

Angle	Male	Male (*n*)	Female	Female (*n*)	*t*	*P*
60°	19.07 ± 3.66	59	16.43 ± 3.11	41	3.758	< 0.001
60°(a)	18.43 ± 1.98	59	16.36 ± 1.30	41	6.290	< 0.001
45°	23.31 ± 1.98	59	20.33 ± 1.49	41	8.167	< 0.001
45°(a)	20.54 ± 2.10	59	18.31 ± 1.62	41	5.724	< 0.001
30°	27.97 ± 2.61	59	24.96 ± 1.83	41	6.378	< 0.001
30°(a)	24.95 ± 2.85	59	22.55 ± 2.17	41	4.553	< 0.001

Continuous data are expressed as mean ± SD. P < 0.05 indicates statistical significance

Discussion

3.1 Clinical Significance and Anatomical Basis of the Insertion Point

This study determined the optimal anchor insertion point at 5.36 ± 1.29 mm proximal to the fibular tip, indicating that the ATFL fibular footprint center lies close to the anteroinferior region of the distal fibula. A systematic review by Matsui et al.[19] reported the ATFL fibular origin to be located 10.0–13.8 mm from the fibular tip along the anterior border. This discrepancy likely reflects differences in reference points, measurement axes, and definitions across studies. Rather than simply replicating prior findings, the present study refines the localization of the ATFL fibular footprint at a quantitative 3D level, offering more actionable anatomical guidance for precise anchor placement. Xie et al.[22] proposed the lowest point of the fibula as a reliable arthroscopic landmark; combining this reference with our quantitative data may further facilitate anatomical repair.

3.2 Determination of Safe Angles and Comparison with Previous Studies

A key finding of this study is the mean maximum safe angle of 67.47 ± 8.05° in the sagittal plane for a 3.0 mm-diameter tunnel to avoid fibular fossa penetration. Although censoring may have underestimated the true θ, it did not affect the conclusions regarding sex-based differences.

Previous studies have approached insertion safety from differing perspectives; however, their measurement reference systems, evaluation objectives, and technical backgrounds were not entirely consistent. Yoshimura et al.[15] recommended an insertion angle of less than 45° to the fibular longitudinal axis to avoid posterior cortical injury. Similarly, Michels et al.[16] advocated a 45° angle,

emphasizing the advantages of oblique tunnels in achieving sufficient length. Liu et al.[11] compared 30°, 45°, and 60° directions and found that 45° offered the best balance among tunnel length, peroneal tendon protection, and distal cortical integrity. In the study by Nakasa et al.[17], the mean drilling angle relative to the anterior fibular border was 59.4°, corresponding to approximately 34.6° relative to the fibular long axis. Most recently, Feng et al.[18] recommended in an evidence-based guideline that fibular-sided insertion be parallel to the sagittal plane, along the fibular longitudinal axis, at 45° to the coronal plane.

The maximum safe angle of approximately 67.5° identified in our study should not be directly conflated with the 45° angle commonly recommended in previous literature. Rather, it represents a further refinement under specific conditions—a defined reference plane, a 3.0 mm tunnel diameter, and fibular fossa penetration as the primary endpoint—supplementing the existing evidence on the safe insertion range for adult ATFL repair.

Importantly, our data reveal a critical interplay between insertion angle and direction. At 60°, the fossa penetration rate was 11.0% in the sagittal plane direction but 0% along the lateral malleolar ridge (60°a), which maintained an effective tunnel length of 17.58 ± 2.01 mm. At the more commonly used 45° and 30°, the sagittal plane direction provided adequate safety (0% penetration) with effective tunnel lengths of 22.09 ± 2.32 mm and 26.74 ± 2.75 mm, respectively—significantly exceeding those of the lateral malleolar ridge direction. Therefore, when intraoperative constraints (e.g., local bony geometry or fracture line orientation) mandate a larger insertion angle, directing the tunnel toward the lateral malleolar ridge is a safer strategy. Under routine conditions, however, insertion at 30°–45° parallel to the sagittal plane optimizes both safety and fixation length. These conclusions are based on imaging and anatomical analyses and warrant further biomechanical and clinical validation.

3.3 Recommendations for Anchor Length Selection

The results underscore the importance of considering sex-related anatomical differences in anchor length selection. The most frequently reported complications of Broström-related procedures include superficial peroneal nerve sensory disturbances and pain from prominent anchors or suture knots[23]. Lee et al.[13] described a case in which even mild posterior anchor prominence caused peroneal tendon irritation and granuloma-like lesions, and noted that the drilling process itself may injure the peroneal tendons.

Complete intraosseous anchor burial is therefore essential. Anchor prominence may abrade adjacent cartilage or tendons and create a palpable subcutaneous prominence. Surgeons should select an anchor length that allows the tail to sit flush with or slightly recessed below the bone surface, and should confirm that no loose knots or suture material remain in the soft tissues. When high-strength tape augmentation is used (e.g., InternalBrace), the tape should also conform closely to the bone surface to avoid a prominent ridge beneath the lateral malleolus[24].

In this study, effective tunnel lengths were significantly greater in males at all tested angles (all $P < 0.001$). At 45° in the sagittal plane direction, for example, the effective tunnel length was 23.31 ± 1.98 mm in males versus 20.33 ± 1.49 mm in females, reflecting larger distal fibular dimensions and greater intraosseous space in males. Based on these findings and commonly available anchor specifications, we recommend anchor lengths not exceeding 20 mm for male patients and 18 mm for female patients. Appropriate anchor selection based on tunnel length helps reduce the risk of anchor tail prominence beyond the bone surface, thereby minimizing irritation to surrounding soft tissues and tendons.

3.4 Limitations

This study has certain limitations. First, although 100 specimens were enrolled, all were derived from single-center imaging data, and the applicability of the results to a broader population requires further validation through multicenter studies. Second, the measurements were based on virtual 3D bone models, reflecting relatively ideal bony conditions; in actual surgical practice, factors such as soft tissue obstruction, ligament remnant quality, bone density variation, and intraoperative technical errors may all affect the final insertion outcome. Third, this study is a quantitative anatomical analysis based on imaging data; the relationship between the "effective tunnel length" and the actual pull-out strength of anchors, as well as the fixation performance corresponding to different insertion angles, remains to be further elucidated through subsequent biomechanical studies. Finally, fibular fossa morphology was not classified in this study, and the specific impact of different morphological variations on insertion safety requires further investigation.

Conclusions

Using virtual 3D reconstruction, this study quantitatively evaluated 100 adult Chinese ankles. The results demonstrated that the optimal ATFL repair insertion point is located approximately 5.4 mm proximal to the fibular tip. Under routine conditions, insertion parallel to the fibular sagittal plane at 30°–45° to the fibular longitudinal axis provides an optimal balance between fibular fossa safety and intraosseous fixation length. When larger angles are unavoidable, the lateral malleolar ridge direction offers a safer alternative. We recommend that anchor length selection account for sex differences, with a maximum length of 20 mm in males and 18 mm for females. These findings may provide a quantitative reference for safe anchor placement in ATFL repair.

Abbreviations

anterior talofibular ligament (ATFL); three-dimensional (3D); fibular obscure tubercle (FOT)

Main text (word count):3526

Abstract (word count):296

References (number):24

Figures (number):2

Tables (number):6

Declarations

Ethics approval and consent to participate:

All experimental protocols were approved by the Ethics Committee of Affiliated Renhe Hospital of China Three Gorges University (Approval No.: RH-2025-EX-022). As this was a retrospective study utilizing anonymized imaging data, the requirement for informed consent was waived by the Ethics Committee of Affiliated Renhe Hospital of China Three Gorges University.

Clinical trial number

Not applicable.

Consent for publication:

Not applicable.

Competing interests:

The authors declare that they have no relevant financial or non-financial interests to disclose.

Funding:

This research received no specific grant from any funding agency.

Author Contribution

ZX-X put forward the conception of the work, designed the study in detail, collected data, conducted the experiments, and drafted the manuscript. JW participated in the experiments and revised the manuscript. ML-C, CY-G, and XQ-C assisted with collecting and analyzing the experimental data. BL revised the manuscript. YZ designed the study in detail, and critically revised and reviewed the manuscript. All authors read and approved the final manuscript.

Acknowledgements:

Not applicable.

Data Availability

The datasets generated and analysed during the current study are available from the corresponding author on reasonable request.

References

1. Liu J, Chen M, Xu T, et al. Functional results of modified Mason-Allen suture versus horizontal mattress suture in the arthroscopic Broström-Gould procedure for chronic ankle instability[J]. J Orthop Surg Res. 2022;17(1):459. 10.1186/s13018-022-03354-4.
2. Song Y, Li H, Sun C, et al. Clinical Guidelines for the Surgical Management of Chronic Lateral Ankle Instability: A Consensus Reached by Systematic Review of the Available Data[J]. Orthop J Sports Med. 2019;7(9):2325967119873852. 10.1177/2325967119873852.
3. Hur ES, Bohl DD, Lee S. Lateral Ligament Instability: Review of Pathology and Diagnosis[J]. Curr Rev Musculoskelet Med. 2020;13(4):494–500. 10.1007/s12178-020-09641-z.
4. Yang H, Su M, Chen Z, et al. Anatomic Measurement and Variability Analysis of the Anterior Talofibular Ligament and Calcaneofibular Ligament of the Ankle[J]. Orthop J Sports Med. 2021;9(11):23259671211047269. 10.1177/23259671211047269.
5. Tsai CS, Huang MT, Jou IM, et al. Arthroscopic modified Broström may improve function while anatomic reconstructions could enhance stability for chronic lateral ankle instability: A network meta-analysis[J]. Foot Ankle Surg. 2024;30(8):630–42. 10.1016/j.fas.2024.05.008.
6. Zhao B, Sun Q, Xu X, et al. Comparison of arthroscopic and open Brostrom-Gould surgery for chronic ankle instability: a systematic review and meta-analysis[J]. J Orthop Surg Res. 2023;18(1):866. 10.1186/s13018-023-04292-5.
7. Attia AK, Taha T, Mahmoud K, et al. Outcomes of Open Versus Arthroscopic Broström Surgery for Chronic Lateral Ankle Instability: A Systematic Review and Meta-analysis of Comparative Studies[J]. Orthop J Sports Med. 2021;9(7):23259671211015207. 10.1177/23259671211015207.
8. Dias S, Lewis TL, Alkhalfan Y, et al. Current concepts in the surgical management of chronic ankle lateral ligament instability[J]. J Orthop. 2022;33:87–94. 10.1016/j.jor.2022.07.006.
9. Mercer NP, Kanakamedala AC, Azam MT, et al. Clinical Outcomes After Suture Tape Augmentation for Ankle Instability: A Systematic Review[J]. Orthop J Sports Med. 2022;10(5):23259671221095791. 10.1177/23259671221095791.
10. Qu F, Ji L, Sun C, et al. Arthroscopic Anterior Talofibular Ligament Repair Combined With All-Inside Suture Tape Augmentation for Treatment of Chronic Lateral Ankle Instability With Generalized Joint

Laxity[J]. Foot Ankle Int. 2024;45(10):1102–10. 10.1177/10711007241271247.

11. Liu C, Zhang Z, Wang J, et al. Optimal fibular tunnel direction for anterior talofibular ligament reconstruction: 45 degrees outperforms 30 and 60 degrees[J]. Knee Surg Sports Traumatol Arthrosc. 2023;31(10):4546–50. 10.1007/s00167-023-07452-6.
12. You G, Huang L, Li M, et al. The safe zone of distal fibula was determined based on the classification of lateral malleolus fossa[J]. J Orthop Surg Res. 2023;18(1):714. 10.1186/s13018-023-04194-6.
13. Lee YK, Lee HS, Cho WJ, et al. Peroneal tendon irritation after arthroscopic modified Broström procedure: A case report[J]. Med (Baltim). 2019;98(51):e18424. 10.1097/MD.0000000000018424.
14. Roward Z, Latt LD. Republication of Fracture Through a Distal Fibular Tunnel Used for an Anatomic Lateral Ankle Ligament Reconstruction[J]. Foot Ankle Orthop. 2023;8(3):24730114231188115. 10.1177/24730114231188115.
15. Yoshimura I, Hagio T, Noda M, et al. Optimal suture anchor direction in arthroscopic lateral ankle ligament repair[J]. Knee Surg Sports Traumatol Arthrosc. 2018;26(7):2110–5. 10.1007/s00167-017-4587-6.
16. Michels F, Matricali G, Guillo S, et al. An oblique fibular tunnel is recommended when reconstructing the ATFL and CFL[J]. Knee Surg Sports Traumatol Arthrosc. 2020;28(1):124–31. 10.1007/s00167-019-05583-3.
17. Nakasa T, Ikuta Y, Ota Y, et al. Safe angles of ATFL and CFL anchor insertion into anatomical attachment of fibula in a lateral ankle ligament repair[J]. J Orthop Sci. 2021;26(1):156–61. 10.1016/j.jos.2020.02.011.
18. Feng SM, Maffulli N, van Dijk CN, et al. All-inside arthroscopic procedures for chronic lateral ankle instability: evidence-based clinical practice guidelines[J]. Br Med Bull. 2025;154(1). 10.1093/bmb/ldaf001.
19. Matsui K, Takao M, Tochigi Y, et al. Anatomy of anterior talofibular ligament and calcaneofibular ligament for minimally invasive surgery: a systematic review[J]. Knee Surg Sports Traumatol Arthrosc. 2017;25(6):1892–902. 10.1007/s00167-016-4194-y.
20. Matsui K, Oliva XM, Takao M, et al. Bony landmarks available for minimally invasive lateral ankle stabilization surgery: a cadaveric anatomical study[J]. Knee Surg Sports Traumatol Arthrosc. 2017;25(6):1916–24. 10.1007/s00167-016-4218-7.
21. Fujishiro H, Nimura A, Azumaya M, et al. Anatomical study of the bone morphology of the anterior talofibular ligament attachment[J]. Anat Cell Biol. 2023;56(3):334–41. 10.5115/acb.23.002.
22. Xie X, Chen L, Fan C, et al. The lowest point of fibula (LPF) could be used as a reliable bony landmark for arthroscopic anchor placement of lateral ankle ligaments ----compared with open Broström procedure[J]. BMC Musculoskelet Disord. 2023;24(1):759. 10.1186/s12891-023-06876-y.
23. Kung JE, Hallman MJ, Humbyrd CJ. Violation of the Subtalar Joint With Novel Suture Tape Augmentation of Lateral Ligament Reconstruction: A Report of 2 Cases[J]. Foot Ankle Orthop. 2022;7(4):24730114221136554. 10.1177/24730114221136554.

24. Pettit DP, Munjal V, Alvarez PM, et al. Arthroscopic Assisted, Lateral Ligament Reconstruction with Suture Tape Augmentation and Knotless All Suture Anchors: A Technique Guide[J]. Arthrosc Tech. 2023;12(11):e2099–103. 10.1016/j.eats.2023.07.033.

Figures

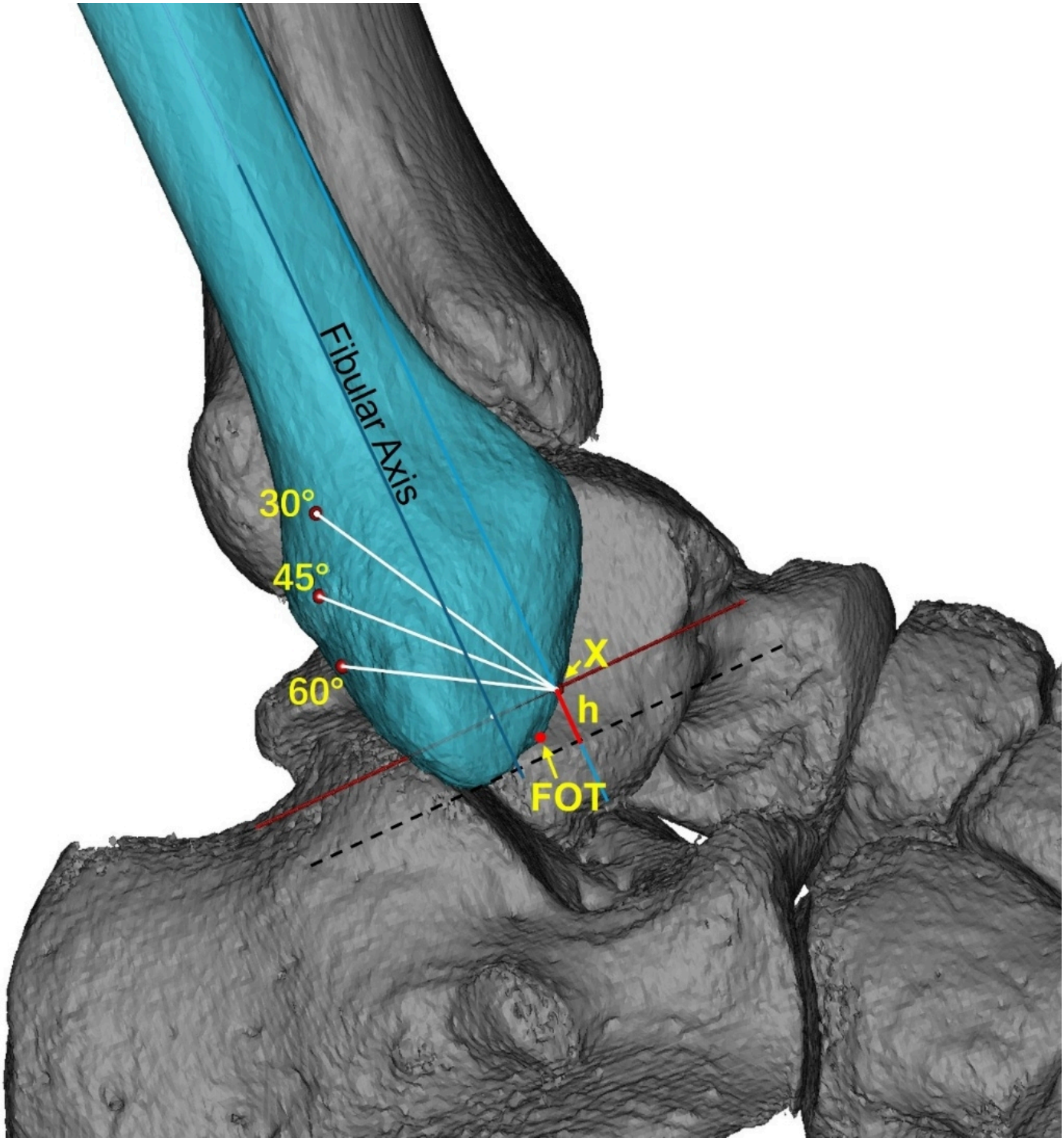


Figure 1

Lateral view of the distal fibula. The fibular anchor tunnels were designed at angles of 30°, 45°, and 60° relative to the fibular longitudinal axis, respectively. Point X, anchor insertion point; FOT, fibular obscure tubercle; h, vertical distance from the insertion point to the fibular tip horizontal plane; dashed line, fibular tip horizontal plane

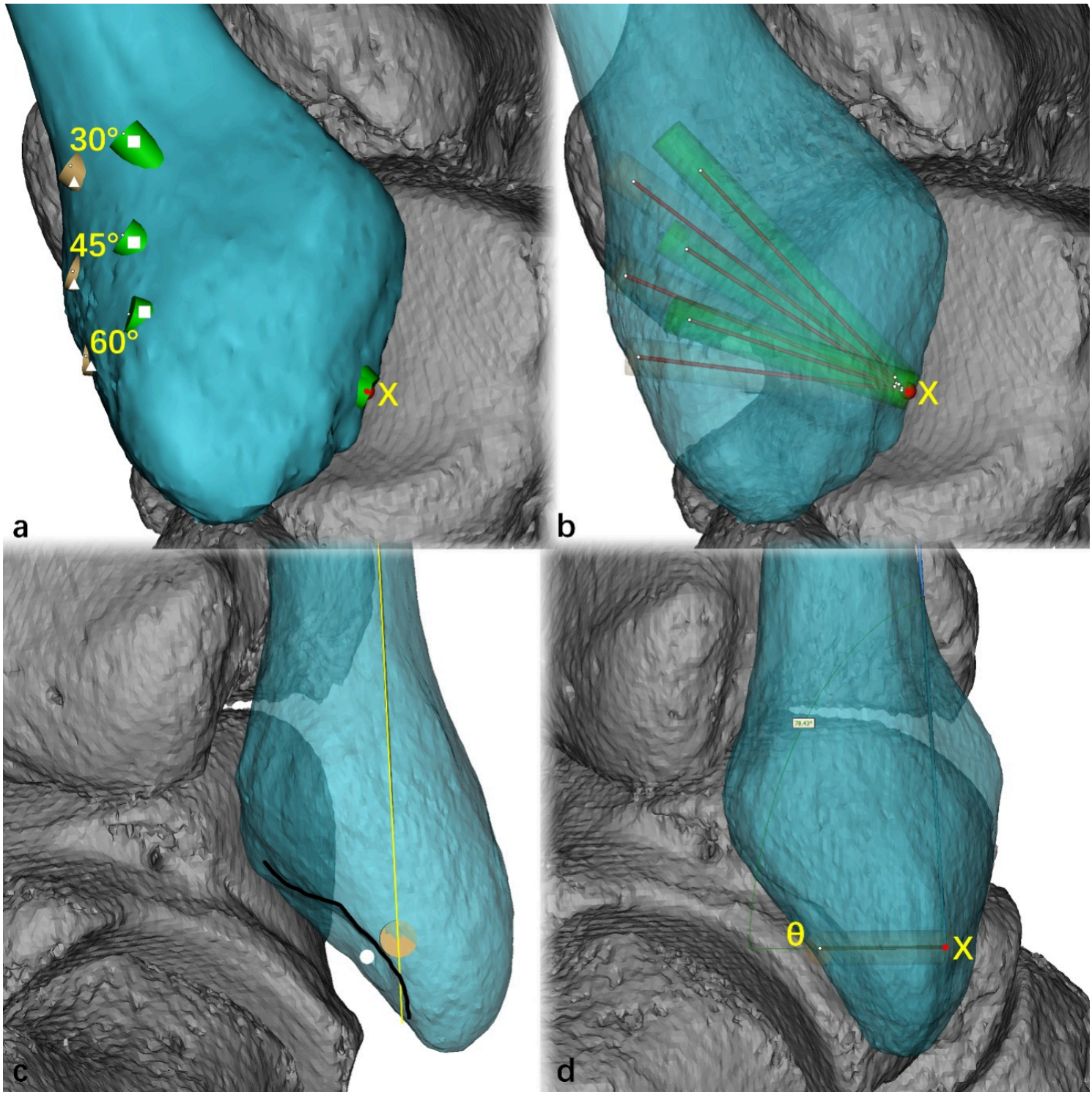


Figure 2

Schematic diagram of simulated fibular-sided anchor insertion and parameter measurement. **a**Tunnel lengths at 60°, 45°, and 30°; X, insertion point; triangles (△), simulated tunnels in the sagittal plane

direction; rectangles (□), simulated tunnels in the lateral malleolar ridge direction. **b** Schematic of the effective tunnel length; line segment, effective tunnel length (i.e., intraosseous fixation length). **c** Simulation of the tunnel at the maximum safe angle in the sagittal plane direction avoiding the fibular fossa; arc, fibular fossa boundary; circle(○), fibular fossa. **d**Measurement of the maximum safe angle in the sagittal plane direction avoiding the fibular fossa